doi: 10.4149/gpb_2024018

A_{2A} adenosine receptor stimulation ameliorated diabetic-induced osteoporosis in rats

Manal S. Abd-El Hamid[1], Ebtessam A. Abou-Shady[1], Nourhan A. Mohamed[1] and Wessam E. Morsy[1]

[1] *Department of Medical Physiology, Faculty of Medicine, Ain Shams University, Cairo, Egypt*

Abstract. Diabetic osteoporosis is a common health problem that is associated with a disruption in bone metabolism. A_{2A} adenosine receptor (A_{2A}AR) signaling seems to play a critical role in bone homeostasis. This study aimed to evaluate the effect of A_{2A}AR stimulation on the treatment of diabetic-induced osteoporosis *versus* insulin treatment. Forty adult male rats were allocated into control (C), untreated diabetic-induced osteoporosis (DIO), insulin-treated DIO (I-DIO), and A_{2A}AR agonist-treated DIO (A-DIO) groups. Both insulin and A_{2A}AR agonist treatments significantly increased serum insulin level, glutathione peroxidase (GPx) activity, bone expression of osteoprotegerin *(Opg)* and β-catenin *(Ctnnb1)*, and cortical and trabecular bone thickness, whereas they decreased serum fasting glucose, malondialdehyde (MDA), tumor necrosis factor α (TNF-α), bone expression of receptor activator of nuclear factor kappa-B ligand *(Rankl),* runt-related transcription factor-2 *(Runx2),* and sclerostin *(Sost) versus* the untreated DIO groups. A_{2A}AR agonist treatment was more effective than insulin in ameliorating diabetic osteoporosis. This might be attributed to the upregulation of β-catenin gene expression, enhancing its anabolic effect on bone, in addition to the A_{2A}AR agonist's anti-oxidative, anti-inflammatory, and anti-diabetic effects.

Key words: A_{2A} adenosine receptor — β-catenin — Diabetes — Osteoporosis

Abbreviations: A_{2A}AR, A_{2A} adenosine receptor; AGEs, advanced glycation end products; BW, body weight; *Ctnnb1,* β-catenin gene; DIO, diabetic-induced osteoporosis; DM, diabetes mellitus; FSG, fasting serum glucose; GLUT2, glucose transporter 2; MDA, malondialdehyde; *Opg,* osteoprotegerin gene; *Rankl,* receptor activator of nuclear factor kappa-B ligand gene; ROS, reactive oxygen species; *Runx2,* runt-related transcription factor-2 gene; *Sost,* sclerostin gene; TNF-α, tumor necrosis factor α; Wnt, wingless-related integration site.

Introduction

The global prevalence of diabetes mellitus (DM) in adults in 2021 was estimated to be 10.5% of the population, with expectations to increase to 12.2% in 2045 (Sun et al. 2022). Long-standing DM is associated with many complications, such as nephropathy, neuropathy, and retinopathy (Chawla et al. 2016). Impaired bone quality and increased fracture risk have become recognized complications of DM (Murray and Coleman 2019). It has been reported that the incidence of osteoporosis exceeds 50% among diabetic patients (Qi et al. 2021).

Diabetic osteoporosis is a systemic metabolic bone disease that might be related to chronic hyperglycemia, oxidative stress, advanced glycation end products (AGEs) accumu-

Correspondence to: Nourhan Abo-Elyazed Mohamed, Department of Medical Physiology, Faculty of Medicine, Ain Shams University, Cairo, Egypt
E-mail: Nourhan_AboElyazed@med.asu.edu.eg

lation, and microvascular changes (Murray and Coleman 2019). Adequate glycemic control is essential for preventing the adverse effects of DM on bone integrity; meanwhile, antidiabetic drugs have a controversial impact on bone health (Adil et al. 2017).

Adenosine is produced both intracellularly and extracellularly from the metabolism of ATP (Manjunath and Sakhare 2009). It regulates many adaptive physiological processes *via* interaction with one or more of four known G-protein-coupled receptors (GPCRs): A_1, A_{2A}, A_{2B}, and A_3 adenosine receptors (ARs) (Sabbadin et al. 2015).

A_{2A}ARs are expressed on bone and might play a role in bone homeostasis (Corciulo and Cronstein 2020). Stimulation of A_{2A}AR diminished inflammatory osteolysis and increased osteoblast numbers in inflamed bone (Mediero et al. 2012). Also, A_{2A}AR activation might restore bone homeostasis by increasing osteoblasts and decreasing osteoclast differentiation, number, and activity (Mediero et al. 2015). Accordingly, A_{2A}AR-deficient mice exhibited low bone density (Mediero et al. 2018). In contrast, Pellegatti et al. (2011) demonstrated that A_{2A}AR drives osteoclast fusion.

In addition, A_{2A}ARs are found in insulin-sensitive tissues such as skeletal muscle and adipose tissue and have been associated with the regulation of glucose homeostasis (Koupenova and Ravid 2013; Csóka et al. 2017). A_{2A}AR deficiency in mice causes decreased insulin production and impaired glucose tolerance in a mouse model of T2DM (Csóka et al. 2017). In an isolated mouse pancreatic islet, adenosine augmented glucose-induced insulin secretion, an effect that was inhibited by A_{2A}AR blockage (Ohtani et al. 2013).

Based on the aforementioned studies, it was intriguing to study the ability of A_{2A}AR agonists to mitigate osteoporosis and bone deterioration in diabetic states.

Materials and Methods

Experimental animals

Forty adult male Wistar rats weighing 180–210 g were purchased from Vacsera Animal House (Helwan), and they were housed in the Medical Ain Shams Research Institute (MASRI), Faculty of Medicine, Ain Sham University, Cairo, Egypt. Rats were kept under standard conditions (12-h light/dark cycle, temperature of 23 ± 2°C) in plastic cages (4 rats/cage) with free access to water and food.

Ethical approval

The study protocol was approved by the Research Ethics Committee, Faculty of Medicine, Ain Shams University (FMASU-REC, MD-90/2020), which conforms to the Guide for the Care and Use of Laboratory Animals published by the US National Institutes of Health. This study is reported according to the ARRIVE guidelines (Animal Research: Reporting of *in vivo* experiment). The sample size was estimated based on a previous bone disease study using the G* Power 3.1.9.7 for Windows (F test), considering an alpha error of 0.05 and 95% power to recognize a 0.9 effect size. The result indicated a minimum of 8 rats *per* group.

Experimental groups

Rats were randomly allocated into 5 groups (8 rats each): control, two untreated diabetic groups and two treated diabetic groups.

1. Control group (**C**): Rats received a single *intraperitoneal* injection (1 ml/kg) of citrate buffer solution (the vehicle of streptozotocin).

Diabetes in diabetic groups was induced in overnight-fasted rats by a single intraperitoneal injection of streptozotocin (STZ) (Sigma-Aldrich, USA), 40 mg/kg/ml, to induce type I DM (Rao et al. 2014; Mostafavinia et al. 2016). STZ was dissolved in freshly prepared sodium citrate buffer (0.1 M, pH 4.5). Three days later, blood glucose was measured using the OK meter-Direct® glucometer (OK Biotech Co. Ltd., Taiwan). Rats whose fasting blood glucose levels were ≥250 mg/dl were considered diabetics (Rao et al. 2014). Then, rats were left for four weeks without treatment after the induction of diabetes to ensure the occurrence of disturbed bone metabolism and to establish a diabetic osteoporosis model (Kim et al. 2017).

Untreated diabetic groups:

2. Diabetic-induced osteoporosis group **$(DIO)_a$**: Diabetic rats didn't receive any further intervention for four weeks.
3. Diabetic-induced osteoporosis group **$(DIO)_b$**: Diabetic rats received daily *intraperitoneal* injections (1 ml/kg) of 10% dimethyl sulfoxide (DMSO) solution (the vehicle of CGS-21680) for four weeks.

Treated diabetic groups:

4. Insulin-treated diabetic-induced osteoporosis group (**I-DIO**): Diabetic rats received daily *subcutaneous* injections of insulin (Humulin 70-30, 100 IU/ml, Lilly, Egypt) at a dose of 10 IU/kg (Rao et al. 2014) for four weeks.
5. A_{2A} adenosine receptor agonist-treated diabetic-induced osteoporosis group (**A-DIO**): Diabetic rats received daily *intraperitoneal* injections of the A_{2A} adenosine receptor agonist (CGS-21680) (TOCRIS Bioscience, Bristol, UK) at a dose of 0.1 mg/kg (Melani et al. 2014) for four weeks.

Experimental procedure

At the end of the study, rats were weighed and anesthetized with an intraperitoneal injection of phenobarbital sodium

(El-Gomhoreya Co., Egypt) at a dose of 40 mg/kg after 8 h of fasting. Blood samples were collected from retro-orbital veins and centrifuged at 4000 rpm for 10 min. The separated serum was then stored at −80°C for subsequent biochemical analysis. Then, the right tibiae were dissected out and stored at −80°C for the determination of quantitative RT-PCR (real-time polymerase chain reaction) studies, whereas the left tibiae were dissected out and fixed in 10% formaldehyde for further histopathological analysis. Researchers were blinded during outcome assessment and data analysis.

Biochemical analysis

Fasting serum glucose, calcium, and phosphorus were measured by the colorimetric method using kits supplied by Elabscience, USA. Serum glutathione peroxidase was measured by the ultraviolet method using a kit supplied by Biodiagnostic, Egypt. Serum malondialdehyde (MDA) was measured by the colorimetric method using a kit supplied by Biodiagnostic, Egypt. Serum levels of insulin, tumor necrosis factor α (TNF-α), and osteocalcin were measured by an enzyme-linked immunosorbent assay (ELISA) technique using Rat ELISA kits supplied by CUSABIO, China, according to the manufacturer's protocol (Cat. No. CSB-E05070r, CSB-E11987r, and CSB-E05129r, respectively).

Quantitative real-time polymerase chain reaction (RT-qPCR)

The rat bone samples were transferred to a pre-chilled RNAlater-ice-filled Eppendorf. The bone samples were meticulously extracted from the RNAlater-ice-filled Eppendorf using sterile forceps. The samples were dissected with a nail nipper to obtain pieces of thickness less than 0.5 cm. Each sample was reweighed to ensure it did not exceed 30 mg. After weighing, the dissected bone tissue was transferred into pre-chilled homogenization tubes containing TRIzol. The homogenate was centrifuged at 12,000 × *g* for 5 min at 4°C. After centrifugation, the clear supernatant containing RNA was cautiously transferred to fresh 2 ml eppendorf tubes. Subsequently, 0.3 ml of chloroform was added to each supernatant tube and vigorously shaken. The samples were centrifuged at 12,000 × *g* for 15 min at 4°C, separating the upper colorless aqueous and lower pink phenol-chloroform phases. The subsequent steps involved the transfer of the aqueous phase and additional centrifugations to isolate the RNA using the RNeasy Mini Kit (Cat. No. 74104, Qiagen, Germany) according to the manufacturer's instructions. RNA was reversely transcribed into complementary DNA (cDNA) using an RT^2 First-Strand Kit (Cat. No. 303404, Qiagen, Germany). SYBR Green-based quantitative real-time PCR amplification and analysis were performed using an Applied Biosystem with software version 3.1 (StepOne™, USA). The relative quantitation was calculated according to Applied Biosystem software using the $2^{-\Delta\Delta Ct}$ method (Livak and Schmittgen 2001) and the results were expressed relative to the gene expression levels in the control group. The primer pair sequences used for each gene are listed as follows: *Rankl* (forward primer: 5'-GACAGCACGCGCTGCTTCTA-3'; reverse primer: 5'-CCACATCGAGCCACGAACCT-3'); *Opg* (forward primer: 5'-GAGTGTGCGAATGTGAGGAA-3'; reverse primer: 5'-AATTAGCAGGAGGCCAAGTG-3'); *Ctnnb1* (forward primer: 5'-CATGGGTGGAACACAGCA-3'; reverse primer: 5'-CCCAGTGCACCCTTCAAC-3'); *Sost* (forward primer: 5'-GCACCATGCAGCTCTCACTA-3'; reverse primer: 5'-GCTGTACTCGGACACGTCTT-3'); *Runx2* (forward primer: 5'-CAGACCAGCAGCAGCACTCCATA-3'; reverse primer: 5'-CGCCAGACAGACTCATCCAT-3').

Histopathological preparation and histomorphometrical analysis

The left tibiae were fixed in 10% formaldehyde for two days. Then they were immersed in a decalcifying agent, a 10% disodium EDTA solution (Elgomhorya Co., Egypt), which was changed daily for 8 weeks. After complete decalcification, all specimens were dehydrated in ascending grades of ethanol. Afterwards, they were stained with hematoxylin and eosin (HandE) (Suvarna et al. 2018), viewed, and analyzed by a light microscope (Zeiss, Germany) equipped with an Axiocam camera.

Cortical and trabecular bone thickness of the left tibiae were determined with histomorphometrical analysis using a computer-mounted Leica Q Win V.3 image analyzer program. The computer was connected to a Leica DM2500 microscope. The trabecular thickness was measured at their midpoint, away from their branching areas at the proximal tibial epiphysis, and the cortical thickness was measured at the mid shaft at objective lens ×10, and the data were reported in μm. Measurements were taken from three different sections obtained from each rat. Three selected non-overlapping fields were examined for each section. The results obtained were averaged to obtain a mean *per* rat for each of the cortical and trabecular bone thicknesses. Then the mean of each group was calculated, and statistical analysis was carried out. All parameters were compiled according to the guidelines of the Nomenclature Committee of the American Society of Bone and Mineral Research (Dempster et al. 2013).

Statistical analysis

Results were expressed as mean ± SEM. Normality was ascertained by the Shapiro-Wilk test. The data were analyzed using SPSS 20.0 software (IBM, Chicago, IL, USA), one-way variance analysis (ANOVA), and least significant difference (LSD). Pearson's correlation coefficient was used to calculate

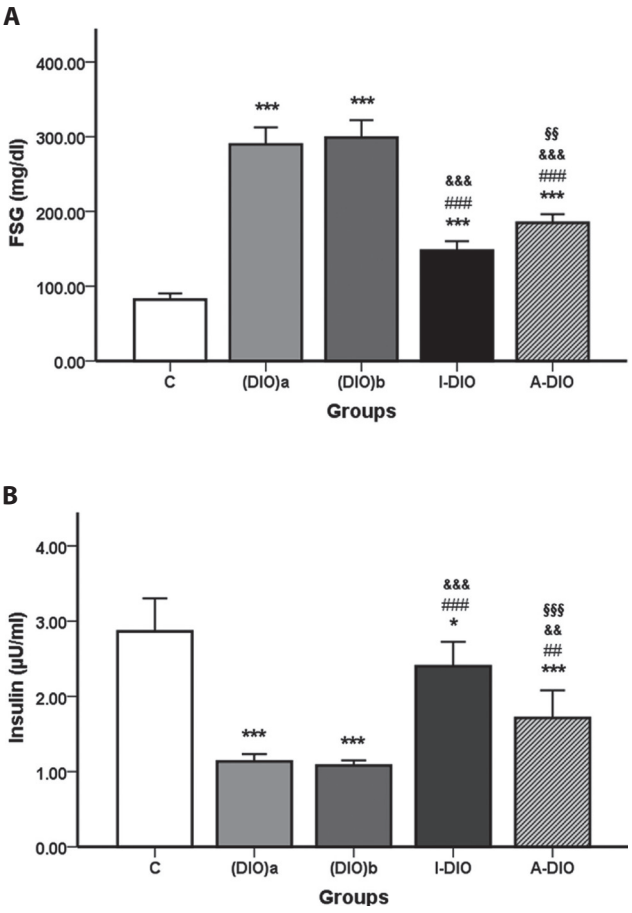

Figure 1. Changes in (**A**) FSG (fasting serum glucose level) and (**B**) serum insulin level. Data are expressed as the mean ± SEM (n = 8). C, control group; $(DIO)_a$, diabetic-induced osteoporosis group a; $(DIO)_b$, diabetic-induced osteoporosis group b – diabetic rats received daily *intraperitoneal* injections (1 ml/kg) of 10% dimethyl sulfoxide (DMSO) solution for four weeks; I-DIO, insulin-treated diabetic-induced osteoporosis group; A-DIO, A_{2A} adenosine receptor agonist-treated diabetic-induced osteoporosis group. * $p < 0.05$, *** $p < 0.001$ *vs.* C group; ## $p < 0.01$, ### $p < 0.001$ *vs.* $(DIO)_a$ group; && $p < 0.01$, &&& $p < 0.001$ *vs.* $(DIO)_b$ group; §§ $p < 0.01$, §§§ $p < 0.001$ *vs.* I-DIO group.

correlations between groups. A p value of <0.05 was considered statistically significant.

Results

Body weight (BW) changes

There were no significant differences in the initial BW between the different groups. Final BW was reduced in the untreated diabetic groups (DIO_a and DIO_b) compared to the control group ($p < 0.001$). Both insulin and CGS-21680 (the $A_{2A}AR$ agonist) treatments increased final BW compared to the untreated diabetic groups ($p < 0.001$ and $p < 0.05$), but were still significantly lower than the control group ($p < 0.001$ for both). There was no significant change detected between the two treated diabetic groups (Table 1).

Glycemic state changes

Untreated diabetic groups showed significantly decreased serum insulin levels and increased fasting serum glucose (FSG) levels compared to the control group ($p < 0.001$ for both). Both insulin and the $A_{2A}AR$ agonist treatments increased serum insulin levels ($p < 0.001$ and $p < 0.01$) and decreased FSG levels ($p < 0.001$ for both). FSG levels were still significantly higher ($p < 0.001$ for both); while serum insulin levels were significantly lower ($p < 0.05$ and $p < 0.001$) in the I-DIO and A-DIO groups compared to the control group. The A-DIO group showed significantly higher FSG levels ($p < 0.01$) and lower serum insulin levels ($p < 0.001$) than the I-DIO group (Fig. 1).

Inflammatory and oxidative stress states

Untreated diabetic groups showed increased serum TNF-α and MDA levels with decreased GPx activity compared to the control group ($p < 0.001$ for all). Both treated diabetic groups showed significant decreases in serum levels of TNF-α and

Table 1. Changes in body weight (BW) and serum levels of osteocalcin, calcium, and phosphorus

Parameter	C (n = 8)	$(DIO)_a$ (n = 8)	$(DIO)_b$ (n = 8)	I-DIO (n = 8)	A-DIO (n = 8)
Initial BW (g)	196.62 ± 3.24	197.50 ± 3.54	194.37 ± 3.76	193.25 ± 2.88	194.62 ± 2.86
Final BW (g)	285.00 ± 3.98	198.62 ± 3.62***	196.50 ± 3.61***	228.25 ± 8.80$^{***,\#\#\#,\&\&\&}$	216.00 ± 5.22$^{***,\#,\&}$
Osteocalcin (pg/ml)	2.78 ± 0.20	9.70 ± 0.75***	10.56 ± 0.96***	5.05 ± 0.45$^{*,\#\#\#,\&\&\&}$	4.01 ± 0.42$^{\#\#\#,\&\&\&}$
Calcium (mg/dl)	10.07 ± 0.15	9.77 ± 0.22	9.89 ± 0.22	9.96 ± 0.19	10.01 ± 0.18
Phosphorus (mg/dl)	4.91 ± 0.15	4.87 ± 0.14	4.99 ± 0.19	4.67 ± 0.13	4.72 ± 0.13

Data are expressed as the mean ± SEM (n = 8). * p <0.05, *** p <0.001 *vs.* C group; # $p < 0.05$, ### $p < 0.001$ *vs.* $(DIO)_a$ group; & $p < 0.05$, &&& $p < 0.001$ *vs.* $(DIO)_b$ group. C, control group; $(DIO)_a$, diabetic-induced osteoporosis group a; $(DIO)_b$, diabetic-induced osteoporosis group b – diabetic rats received daily intraperitoneal injections (1 ml/kg) of 10% dimethyl sulfoxide (DMSO) solution for four weeks; I-DIO, insulin-treated diabetic-induced osteoporosis group; A-DIO, A_{2A} adenosine receptor agonist-treated diabetic-induced osteoporosis group.

MDA, with a significant increase in GPx activity compared to the untreated diabetic groups ($p < 0.001$ for all). Serum TNF-α and GPx activity were still significantly different from the control, whereas serum MDA reached the control level. No significant changes were observed between the I-DIO and A-DIO groups (Fig. 2).

Serum levels of osteocalcin, calcium, and phosphorus

Serum osteocalcin levels were significantly higher in the untreated diabetic groups compared to the control group ($p < 0.001$). I-DIO and A-DIO groups showed significant decreases in serum osteocalcin levels compared to the untreated diabetic groups ($p < 0.001$ for both). Compared to the control group, serum osteocalcin levels were non-significantly different from those in the A-DIO group while still significantly higher in the I-DIO group ($p < 0.05$). The treated diabetic groups were not significantly different from each other. Serum calcium and phosphorus levels showed non-significant changes in all studied groups (Table 1).

Bone Opg and Rankl expressions and the Rankl/Opg ratio

A significant decrease in *Opg* and a significant increase in *Rankl* relative expression and the *Rankl/Opg* ratio were observed in the untreated diabetic rat's tibia compared to the control group ($p < 0.001$ for all).

Opg relative expression significantly increased after treatment with either insulin or CGS-21680 compared to the untreated diabetic groups, whereas *Rankl* relative expression and the *Rankl/Opg* ratio decreased ($p < 0.001$ for all).

Compared to the control group, in both treated groups, *Opg* was still significantly lower ($p < 0.001$), and the *Rankl/Opg* ratio was not significantly changed. *Rankl* relative expression was still significantly higher ($p < 0.01$) in the I-DIO group, while it was comparable to the control group in A-DIO.

The A-DIO group showed a significant decrease in *Rankl* relative expression and an increase in *Opg* relative expression ($p < 0.05$ for both) when compared to the I-DIO group; however, the *Rankl/Opg* ratio was non-significantly different. (Fig. 3A–C)

Changes in bone Runx2, Ctnnb1, and Sost expressions

In untreated diabetic groups, the relative expressions of *Runx2* and *Sost* were increased while that of *Ctnnb1* was decreased compared to the control group ($p < 0.001$). After treatment with insulin or CGS-21680, there was a significant decrease in *Runx2* and *Sost* and an increase in *Ctnnb1* relative expression ($p < 0.001$ for all) that were still significantly different compared to the control group. A significant increase in *Ctnnb1* relative expression was observed in the A-DIO group compared to the I-DIO group ($p < 0.05$), with no significant difference detected between them regarding *Runx2* and *Sost* relative expressions (Fig. 3D–F).

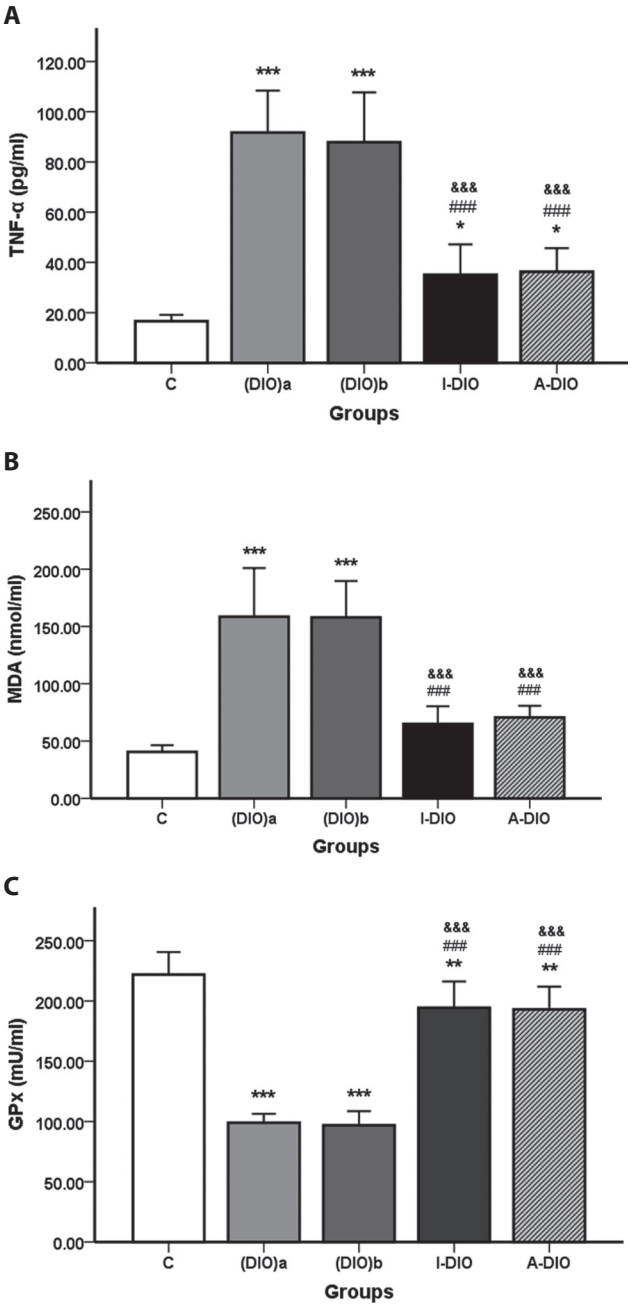

Figure 2. Changes in (**A**) serum TNF-α (tumor necrosis factor α), (**B**) serum malondialdehyde (MDA), and (**C**) serum glutathione peroxidase (GPx) in different studied groups. Data are expressed as the mean ± SEM ($n = 8$). * $p < 0.05$, ** $p < 0.01$, *** $p < 0.001$ *vs.* C group; ### $p < 0.001$ *vs.* $(DIO)_a$ group; &&& $p < 0.001$ *vs.* $(DIO)_b$ group. For more abbreviations, see Figure 1.

Effect on bone microarchitecture

In the control rats, HandE-stained longitudinal sections of the tibia revealed average cortical thickness with a regular meshwork of trabecular bone (Fig. 4A).

The cortical bone thickness of the untreated diabetic rats became thinner with irregularly eroded bony trabeculae (Fig. 4A).

Following insulin or CGS-21680 treatment, cortical bone thickness increased with well-organized bone lamellae and well-developed bone trabeculae (Fig. 4A).

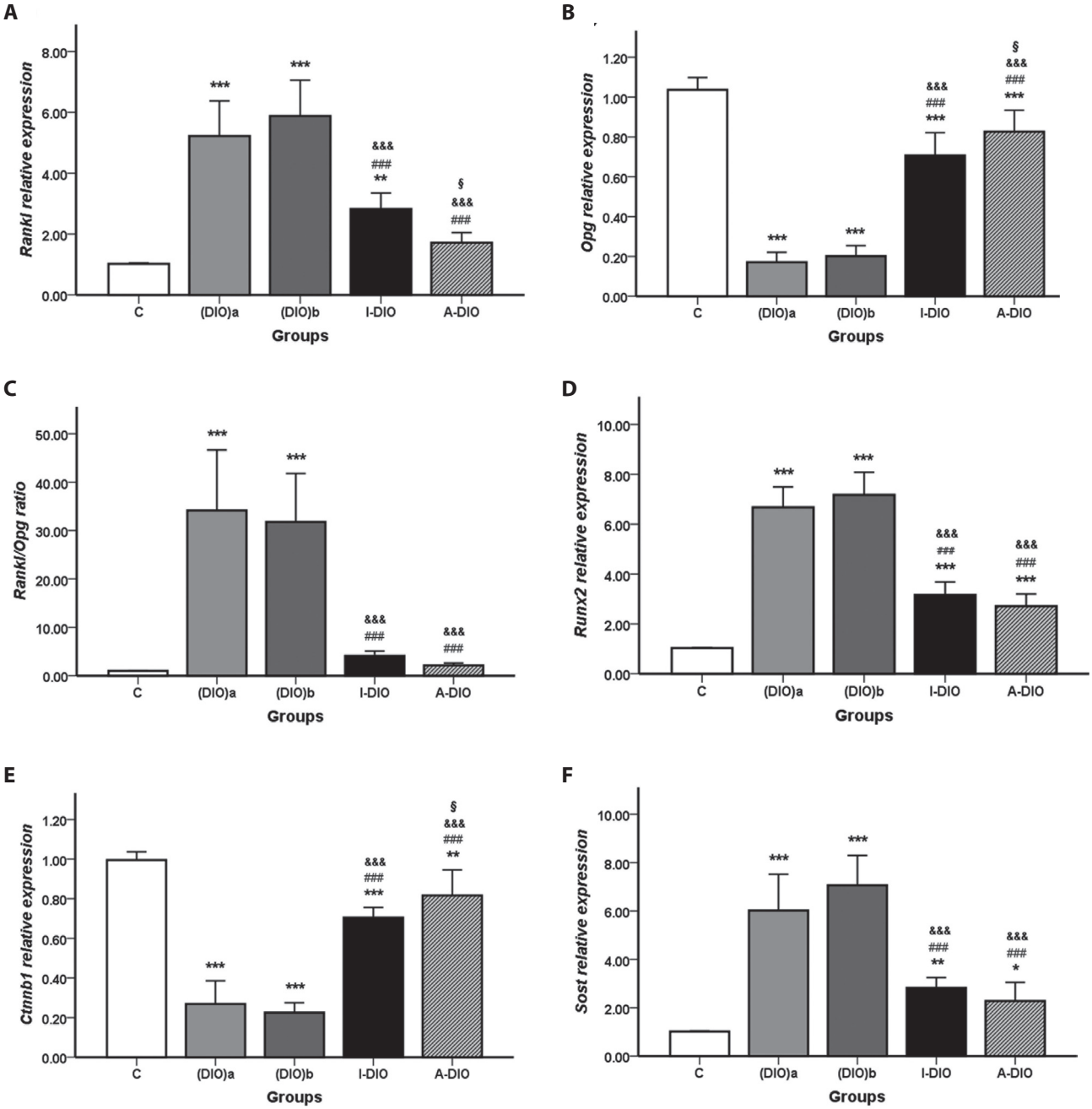

Figure 3. Relative expression levels of: (**A**) *Rankl* (receptor activator of nuclear factor kappa-B ligand), (**B**) *Opg* (osteoprotegerin), (**C**) *Rankl/Opg* ratio, (**D**) *Runx2 (*receptor activator of nuclear factor kappa-B ligand), (**E**) *Ctnnb1* (β-catenin), and (**F**) *(Sost)* sclerostin in rat's tibia. Data are expressed as the mean ± SEM ($n = 8$). * $p < 0.05$, ** $p < 0.01$, *** $p < 0.001$ *vs.* C group; ### $p < 0.001$ *vs.* $(DIO)_a$ group; &&& $p < 0.001$ *vs.* $(DIO)_b$ group; § $p < 0.05$ *vs.* I-DIO group. For more abbreviations, see Figure 1.

In histomorphometry, cortical and trabecular bone thickness showed a significant decrease ($p < 0.001$ for all) in the untreated diabetic groups compared to the control group. These parameters were significantly increased in the treated groups ($p < 0.001$ for all) compared to the untreated diabetic groups. They were still significantly lower than the control group ($p < 0.001$ for both) in the I-DIO group but reached the control values in the A-DIO group (Fig. 4B,C).

Correlation studies

As shown in Table 2, FSG, serum TNF-α, and MDA levels showed a significant positive correlation with *Rankl* and *Sost* relative expressions ($p < 0.001$), while they showed a significant negative correlation with *Opg* and *Ctnnb1* relative expressions ($p < 0.001$) and tibial cortical and trabecular bone thickness ($p < 0.001$). Moreover, a significant positive correlation was detected between fasting serum glucose and both serum MDA and TNF-α.

Ctnnb1 relative expression was positively correlated with *Opg* relative expression, while it was negatively correlated with *Rankl, Runx2*, and *Sost* relative expressions. There was a significant positive correlation between *Rankl, Runx2*, and *Sost* relative expressions ($p < 0.001$). *Opg* relative expression correlated negatively with *Rankl, Runx2*, and *Sost* relative expressions (Table 2).

Tibial cortical and trabecular bone thickness were negatively correlated with *Rankl, Runx2*, and *Sost* relative expressions, while they were positively correlated with *Opg* and *Ctnnb1* relative expressions ($p < 0.001$) (Table 2).

Discussion

The present study demonstrated the effects of A_{2A}AR stimulation on bone integrity in a type 1 diabetic-induced osteoporosis model in comparison to insulin treatment.

STZ is cytotoxic to β-cells; it is taken up by pancreatic β-cells *via* the GLUT2 transporter, where it causes β-cell death by DNA fragmentation, leading to hyperglycemia (Eleazu et al. 2013). This hyperglycemia can increase mitochondrial production of reactive oxygen species (ROS), leading to intracellular oxidative stress and inflammation with consequent β-cell dysfunction and death (Tangvarasittichai 2015; Li and Shen 2019). In the present study, both insulin and the A_{2A}AR agonist improved the glycemic state, which might halt further β-cell dysfunction that results from mitochondrial glucotoxicity (Wu and Yan 2015). The improvement in glycemic state in the A_{2A}AR-agonist-treated diabetic group can be attributed to the antioxidant and anti-inflammatory effects of the A_{2A}AR signaling, as evidenced by the decreased serum MDA and TNF-α levels and the increased serum GPx activity. Also, fasting serum glucose levels were significantly positively correlated with serum MDA and TNF-α levels and negatively correlated with serum GPx activity. This is consistent with previous stud-

Table 2. Correlations between glycemic indices, oxidative stress, inflammatory markers, bone-regulating gene relative expressions, and bone histomorphometry

		FSG	*Rankl*	*Opg*	*Runx2*	*Ctnnb1*	*Sost*	Ct Th	Tb Th
FSG	r	1	0.85	−0.89	0.93	−0.87	0.85	−0.78	−0.86
	p		≤0.001	≤0.001	≤0.001	≤0.001	≤0.001	≤0.001	≤0.001
TNF-**α**	r	0.87	0.86	−0.86	0.85	−0.84	0.77	−0.80	−0.85
	p	≤0.001	≤0.001	≤0.001	≤0.001	≤0.001	≤0.001	≤0.001	≤0.001
MDA	r	0.82	0.68	−0.83	0.87	−0.81	0.76	−0.73	−0.78
	p	≤0.001	≤0.001	≤0.001	≤0.001	≤0.001	≤0.001	≤0.001	≤0.001
Rankl	r	0.85	1	−0.87	0.85	−0.84	0.81	−0.82	−0.85
	p	≤0.001		≤0.001	≤0.001	≤0.001	≤0.001	≤0.001	≤0.001
Opg	r	−0.89	−0.87	1	−0.93	0.93	−0.85	0.86	0.90
	p	≤0.001	≤0.001		≤0.001	≤0.001	≤0.001	≤0.001	≤0.001
Runx2	r	0.93	0.85	−0.93	1	−0.91	0.91	−0.85	−0.89
	p	≤0.001	≤0.001	≤0.001	≤0.001	≤0.001	≤0.001	≤0.001	≤0.001
Ctnnb1	r	−0.87	−0.84	0.93	−0.91	1	−0.88	0.90	0.93
	p	≤0.001	≤0.001	≤0.001	≤0.001		≤0.001	≤0.001	≤0.001
Sost	r	0.85	0.81	−0.85	0.91	−0.88	1	−0.82	−0.84
	p	≤0.001	≤0.001	≤0.001	≤0.001	≤0.001		≤0.001	≤0.001

Data are expressed as r values. FSG, fasting serum glucose; TNF-α, tumor necrosis factor α; MDA, malondialdehyde; *Rankl,* receptor activator of nuclear factor kappa-B ligand, *Opg,* osteoprotegerin; *Runx2*, runt-related transcription factor-2; *Ctnnb1,* β-catenin; *Sost,* sclerostin; Ct Th, cortical thickness; Tb Th, trabecular thickness.

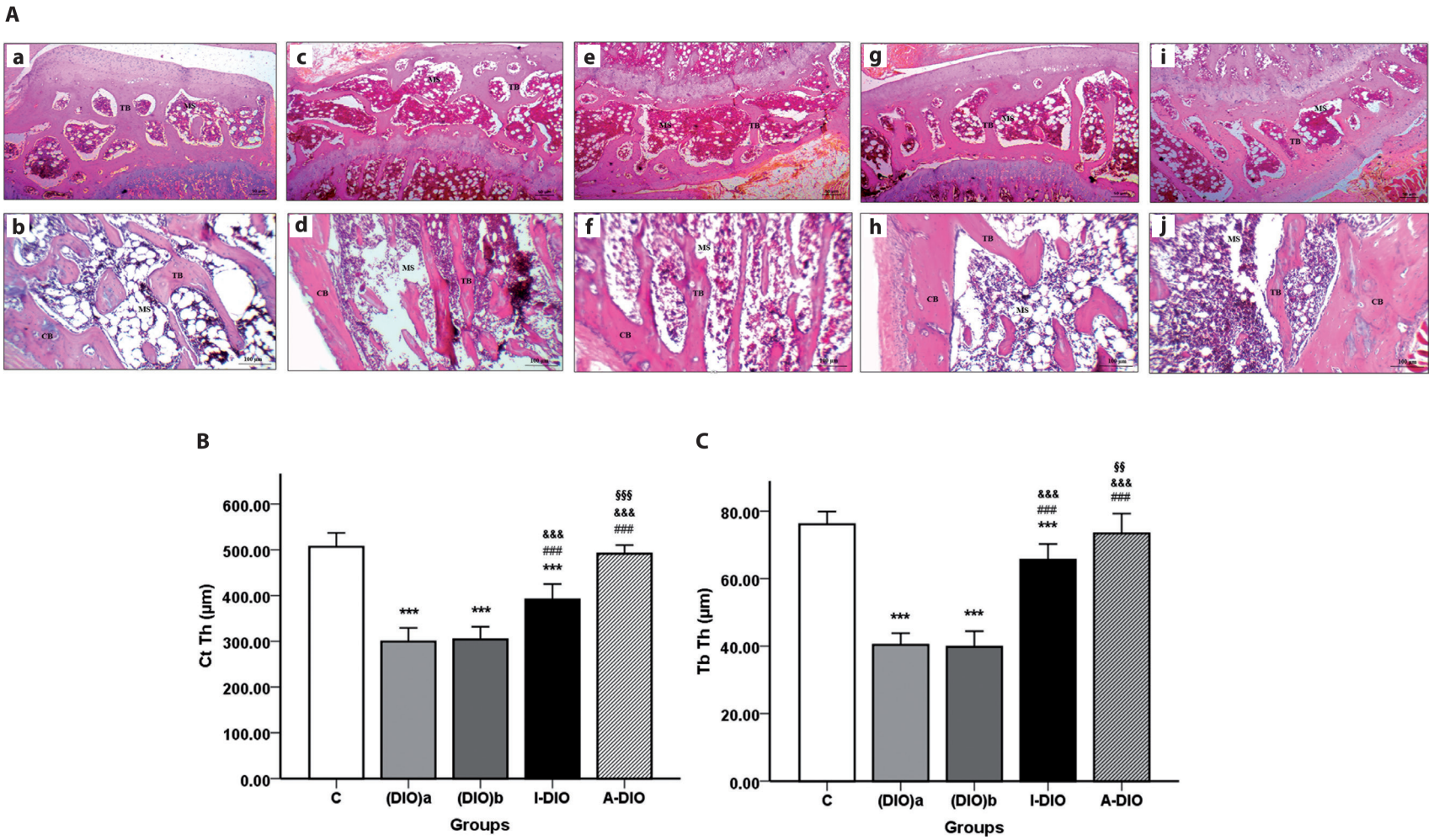

Figure 4. A. Photomicrographs of longitudinal sections of the proximal tibial epiphysis of rats showing cortical and trabecular bone by HandE staining. **a., b.** Control group: bone showing average cortical bone (CB) thickness with average bone density, intact well-formed dense trabecular bone (TB) and average intervening bone marrow spaces (MS). **c., d.** $(DIO)_a$ group: bone showing thin cortical bone (CB) with poorly mineralized areas and thin eroded trabecular bone (TB) with wide bone marrow spaces (MS). **e., f.** ($DIO)_b$ group: bone showing thin cortical bone (CB), with thin trabecular bone (TB), and wide bone marrow spaces (MS). **g., h.** I-DIO group: bone showing thin faint cortical bone (CB) and thin trabecular bone (TB). **i., j.** A-DIO group: bone showing thick faint cortical bone (CB) with areas of ossifying cartilage and relatively thin trabecular bone (TB). Top row (a, c, e, g, i): magnification ×40, scale bar: 50 µm; bottom row (b, d, f, h, j): magnification ×200, scale bar: 100 µm. **B.** Bone cortical thickness (Ct Th) in rat's tibia. **C.** Trabecular thickness (Tb Th) in rat's tibia. Data are expressed as the mean ± SEM ($n = 8$). *** $p < 0.001$ *vs.* C group; ### $p < 0.001$ *vs.* $(DIO)_a$ group; &&& $p < 0.001$ *vs.* $(DIO)_b$ group; §§ $p < 0.01$, §§§ $p < 0.001$ *vs.* I-DIO group. For more abbreviations, see Figure 1.

ies that demonstrated that A_{2A}AR stimulation can inhibit the generation of ROS, reduce DNA damage, and oxidative stress-induced apoptosis through a cAMP/PKA-dependent pathway (Nadeem et al. 2007; Chiu et al. 2015). In the same context, Kong et al. reported an increase in GPx activity after A_{2A}AR agonist administration in a rat model of inflammatory lung disease (Kong et al. 2019).

In addition, the recorded improvement of bone metabolism in the present study, indicated by the increased expression of *Opg* and the decreased expression of *Rankl* and *Sost*, can explain the beneficial effect of A_{2A}AR stimulation on glycemic state. Recent advances in bone biology have highlighted the importance of bone as an endocrine organ that might regulate insulin signaling and glucose tolerance (Faienza et al. 2015). Fasting serum glucose level was positively correlated with *Rankl* and Sost relative expressions and negatively correlated with *Opg* relative expression. This goes with the Xiang et al. (2023) suggestion that inhibition of RANKL, a bone resorping marker, improved hepatic insulin sensitivity and affected β-cell function. Also, sclerostin-deficient mice exhibited a reduction in white adipose tissue accumulation, along with corresponding enhancements in glucose and fatty acid metabolism and increased insulin sensitivity (Kim et al. 2017). Similarly, *in vitro*, osteoprotegerin (OPG) treatment of pancreatic β-cell lines decreased insulin release following glucose stimulation, thus preventing exhaustion of β-cell function (Kuroda et al. 2016). Furthermore, A_{2A}AR activation might stimulate β-cell proliferation and regeneration (Andersson et al. 2012).

Therefore, the improvement in the oxidative stress and inflammatory states and the bone metabolic markers in the A_{2A}AR-agonist-treated group could be the underlying mechanisms that improved the glycemic state in this group.

The STZ-induced hypoinsulinemia in untreated diabetic rats resulted in the wasting of fat stores, which explained the significant decrease in BW gain in diabetic groups (Howarth et al. 2005). Insulin treatment partially recovered BW owing to its ability to inhibit protein catabolism, stimulate lipogenesis, and slow basal metabolism (Mottalib et al. 2017). Despite previous claims that adenosine agonists might activate lipolysis and increase energy expenditure (DeOliveira et al. 2017), in this study, CGS-21680 reduced weight loss, which may be related to the improvement in serum insulin levels.

In this study, the untreated diabetic rats showed deterioration in bone microarchitecture. Insulin and the A_{2A}AR agonist treatments promoted bone regeneration. These protective effects can be mediated by either enhancing osteoblastogenesis or inhibiting osteoclastogenesis.

To understand the mechanisms by which insulin and the A_{2A}AR agonist restored bone microarchitecture, we investigated RANK/RANKL/OPG and the canonical Wnt/β-catenin pathways.

The RANK/RANKL/OPG signaling pathway is involved in the process of osteoclastogenesis. RANKL can bind to its receptor, RANK, on osteoclasts and stimulate their maturation and differentiation (Zhao et al. 2020). The action of RANKL is blocked by OPG, which prevents the binding of RANKL to the RANK receptor, inhibiting bone resorption (Domazetovic et al. 2017), whereas β-catenin, a central component in the canonical Wnt signaling pathway, plays an important role in osteoblastogenesis (Borhani et al. 2019).

In the current study, insulin and the A_{2A}AR agonist treatments upregulate *Ctnnb1* and *Opg* expressions, whereas they downregulate *Rankl* and *Sost*, a Wnt antagonist, and decrease the *Rankl*/*Opg* ratio, an index of bone resorption (Domazetovic et al. 2017).

A_{2A}AR activation increases cellular β-catenin levels and enhances its phosphorylation to deliver signals critical for bone formation (Borhani et al. 2019). β-catenin has also been reported to promote the production of OPG, thus inhibiting osteoclastogenesis (Kurgan et al. 2019). Herein, *Ctnnb1* expression was positively associated with *Opg* expression and negatively correlated with *Rankl* expression. In addition, cortical and trabecular bone thickness were positively associated with *Ctnnb1* and *Opg* expressions, while they were negatively associated with *Rankl* and *Sost* expressions. In agreement with this study, increased bone cortical and trabecular thickness, bone regeneration, and healing were linked to insulin (Nyman et al. 2017) and A_{2A}AR stimulation (Mediero et al. 2015).

Therefore, the significant increase in β-catenin gene expression in the treated groups may mediate the bone improvement. This crosstalk between insulin, A_{2A}AR, and Wnt/β-catenin signaling goes in line with previous studies that showed the ability of insulin (Cabrae et al. 2020) and A_{2A}AR signaling (Zhang et al. 2017; Borhani et al. 2019) to activate the Wnt/β-catenin pathway.

The improvement in diabetic-induced osteoporosis could also be attributed to the reduction in blood glucose or the restoration of the anabolic effect of insulin on bone (Gomes et al. 2019). Hyperglycemia exerts an inhibitory effect on the canonical Wnt pathway by upregulating *Sost* expression in osteocytes (Pacicca et al. 2019). In this study, FSG was positively associated with *Rankl* and *Sost* expressions and negatively associated with *Ctnnb1* and *Opg* expressions.

Furthermore, the improvement in hyperglycemia-associated oxidative stress and inflammation denoted by the significant decrease in serum MDA and TNF-α levels, together with the increased GPx activity in the insulin and A_{2A}AR agonist-treated groups, could also explain the mitigation of osteoporotic changes induced by DM. ROS reduce osteoblast activity and their rate of OPG production (Romagnoli et al. 2013), induce apoptosis in osteoblasts, and reduce their differentiation ability (Ma et al. 2014). Apoptotic osteoblasts and osteocytes produce high levels of sclerostin, which blocks

OPG synthesis by inhibiting the Wnt/β-catenin pathway in these cells and impairing bone formation (Pietrzyk et al. 2017). In addition, ROS activates the differentiation of pre-osteoclasts into osteoclasts by upregulating *Rankl* expression and downregulating *Opg* expression (Fontani et al. 2015). Furthermore, increased TNF-α levels due to hyperglycemia may impair osteoblast proliferation and stimulate osteoblast apoptosis (Costantini and Conte 2019; Qi et al. 2021). TNF-α acts as a pro-resorptive factor as it stimulates RANKL expression in osteoblasts (Murray and Coleman 2019). In the present study, both MDA and TNF-α serum levels were positively correlated with *Rankl* and *Sost* expressions and were negatively correlated with *Ctnnb1* and *Opg* expression and both cortical and trabecular bone thickness. Therefore, the anti-oxidative and anti-inflammatory effects of insulin (Sun et al. 2014) and the A_{2A}AR agonist (Kong et al. 2019) mitigated bone resorption.

Elevated serum osteocalcin levels and *Runx2* expression in the untreated diabetic groups, although they are indicators of osteoblast differentiation (Costantini and Conte 2019), reflected increased osteoclastic bone resorption with leakage of a large fraction of osteocalcin into the systemic circulation (Greenblatt et al. 2017) and a high bone turnover state with an attempted compensatory response.

Haxaire et al. (2016) demonstrated that overexpression of *Runx2* inhibits the canonical Wnt/β-catenin pathway, down-regulates *Opg*, and upregulates *Rankl* expression, increasing the *Rankl*/*Opg* ratio in cells of the osteoblastic lineage and hence enhancing bone resorption. Similarly, in this study, *Runx2* expression showed a negative correlation with *Opg* expression and a positive correlation with *Rankl* expression. Both insulin and the A_{2A}AR agonist restored serum osteocalcin and *Runx2* expression levels. The insignificant differences between serum calcium and phosphorus in spite of increased bone resorption in the untreated diabetic groups could result from osmotic diuresis in hyperglycemic states (Yang et al. 2020).

Conclusion

A_{2A}AR agonist treatment can ameliorate diabetic-induced osteoporosis. This osteoanabolic effect could be mediated, in part, *via* enhancing β-catenin gene expression, with consequent upregulation of *Opg* and downregulation of *Rankl* gene expression, as well as the anti-oxidative and anti-inflammatory effects of A_{2A}AR activation, which dampen inflammatory bone destruction. In addition, the improvements in bone metabolism may favor glycemic control. Therefore, A_{2A}AR stimulation may serve as a promising agent for controlling osteoporotic bone changes in diabetic patients.

Conflict of interest. All authors have no conflicts of interest.

Acknowledgement. The authors acknowledge Dr. Sayed Abdel-Raheem, Assistant Professor of Histopathology at Al Azhar Faculty of Medicine, Cairo; Dr. Eman Hamdy, Lecturer of Histopathology at Faculty of Medicine, Ain Shams University, Cairo, for scientific help in the histopathological assessment; Dr. Laila Rashed, Professor of Medical Biochemistry and Molecular Biology at Faculty of Medicine, Cairo University, for assistance in biochemical analysis, and Nabila Mohammed, Assistant Lecturer of Epidemiology at Community, Environmental, and Occupational Medicine at Faculty of Medicine, Ain Shams University, Cairo, for scientific help in the statistical analysis.

Author contributions. Ebtessam A. Abou-Shady, Wessam E. Morsy, and Manal S. Abd El-Hamid designed the study. Manal S. Abd-El Hamid, Wessam E. Morsy, and Nourhan A. Mohamed performed the practical steps of this work. All authors analyzed and interpreted the data, contributed to the writing of the manuscript, and revised and approved the final manuscript.

References

Adil M, Khan RA, Kalam A, Venkata SK, Kandhare AD, Ghosh P, Sharma M (2017): Effect of anti-diabetic drugs on bone metabolism: Evidence from preclinical and clinical studies. Pharmacol. Rep. **69,** 1328-1340 https://doi.org/10.1016/j.pharep.2017.05.008

Andersson O, Adams BA, Yoo D, Ellis GC, Gut P, Anderson RM, German MS, Stainier DY (2012): Adenosine signaling promotes regeneration of pancreatic β cells in vivo. Cell Metab. **15,** 885-894 https://doi.org/10.1016/j.cmet.2012.04.018

Borhani S, Corciulo C, Larranaga-Vera A, Cronstein BN (2019): Adenosine A2A receptor (A2AR) activation triggers Akt signaling and enhances nuclear localization of β-catenin in osteoblasts. FASEB J. **33,** 7555 https://doi.org/10.1096/fj.201900014R

Cabrae R, Dubuquoy C, Caüzac M, Morzyglod L, Guilmeau S, Noblet B, Fève B, Postic C, Burnol AF, Moldes M (2020): Insulin activates hepatic Wnt/β-catenin signaling through stearoyl-CoA desaturase 1 and Porcupine. Sci. Rep. **10,** 5186 https://doi.org/10.1038/s41598-020-61869-4

Chawla A, Chawla R, Jaggi S (2016): Microvasular and macrovascular complications in diabetes mellitus: distinct or continuum? Indian J. Endocrinol. Metab. **20,** 546 https://doi.org/10.4103/2230-8210.183480

Chiu FL, Lin JT, Chuang CY, Chien T, Chen CM, Chen KH, Hsiao HY, Lin YS, Chern Y, Kuo HC (2015): Elucidating the role of the A2A adenosine receptor in neurodegeneration using neurons derived from Huntington's disease iPSCs. Hum. Mol. Genet. **24,** 6066-6079 https://doi.org/10.1093/hmg/ddv318

Corciulo C, Cronstein BN (2020): Signaling of the purinergic system in the joint. Front. Pharmacol. **10,** 1591 https://doi.org/10.3389/fphar.2019.01591

Costantini S, Conte C (2019): Bone health in diabetes and prediabetes. World J. Diabetes **10,** 421 https://doi.org/10.4239/wjd.v10.i8.421

Csóka B, Törő G, Vindeirinho J, Varga ZV, Koscsó B, Németh ZH, Kókai E, Antonioli L, Suleiman M, Marchetti P, et al. (2017): A2A adenosine receptors control pancreatic dysfunction in high-fat-diet-induced obesity. FASEB J. **31,** 4985 https://doi.org/10.1096/fj.201700398R

Dempster DW, Compston JE, Drezner MK, Glorieux FH, Kanis JA, Malluche H, Meunier PJ, Ott SM, Recker RR, Parfitt AM (2013): Standardized nomenclature, symbols, and units for bone histomorphometry: a 2012 update of the report of the ASBMR Histomorphometry Nomenclature Committee. J. Bone Min. Res. **28,** 2 https://doi.org/10.1002/jbmr.1805

DeOliveira CC, Gotardo EM, Ribeiro ML, Gambero A (2017): Role of A1 and A2A adenosine receptor agonists in adipose tissue inflammation induced by obesity in mice. Eur. J. Pharmacol. **799,** 154-159 https://doi.org/10.1016/j.ejphar.2017.02.017

Domazetovic V, Marcucci G, Iantomasi T, Brandi ML, Vincenzini MT (2017): Oxidative stress in bone remodeling: role of antioxidants. Clin. Cases Miner. Bone Metab. **14,** 209 https://doi.org/10.11138/ccmbm/2017.14.1.209

Eleazu CO, Eleazu KC, Chukwuma S, Essien UN (2013): Review of the mechanism of cell death resulting from streptozotocin challenge in experimental animals, its practical use and potential risk to humans. J. Diabetes Metab. Disord. **12,** 1-7 https://doi.org/10.1186/2251-6581-12-60

Faienza MF, Luce V, Ventura A, Colaianni G, Colucci S, Cavallo L, Grano M, Brunetti G (2015): Skeleton and glucose metabolism: a bone-pancreas loop. Int. J. Endocrinol. **2015,** 758148 https://doi.org/10.1155/2015/758148

Fontani F, Marcucci G, Iantomasi T, Brandi ML, Vincenzini M T (2015): Glutathione, N-acetylcysteine and lipoic acid down-regulate starvation-induced apoptosis, RANKL/OPG ratio and sclerostin in osteocytes: involvement of JNK and ERK1/2 signalling. Calcif. Tissue Int. **96,** 335-346 https://doi.org/10.1007/s00223-015-9961-0

Gomes GJ, Carlo RJ, Silva MF, Cunha DN, Silva ED, Silva KA, Carneiro-Junior MA, Prímola-Gomes TN, Natali AJ (2019): Swimming training potentiates the recovery of femoral neck strength in young diabetic rats under insulin therapy. Clinics **74,** e829 https://doi.org/10.6061/clinics/2019/e829

Greenblatt MB, Tsai JN, Wein MN (2017): Bone turnover markers in the diagnosis and monitoring of metabolic bone disease. Clin. Chem. **63,** 464-474 https://doi.org/10.1373/clinchem.2016.259085

Haxaire C, Haÿ E, Geoffroy V (2016): Runx2 controls bone resorption through the down-regulation of the Wnt pathway in osteoblasts. Am. J. Pathol. **186,** 1598-1609 https://doi.org/10.1016/j.ajpath.2016.01.016

Howarth FC, Jacobson M, Shafiullah M, Adeghate E (2005): Long-term effects of streptozotocin-induced diabetes on the electrocardiogram, physical activity and body temperature in rats. Exp. Physiol. **90,** 827-835 https://doi.org/10.1113/expphysiol.2005.031252

Kim HJ, Jung BH, Yoo KY, Han JW, Um HS, Chang BS, Lee JK (2017): Determination of the critical diabetes duration in a streptozotocin-induced diabetic rat calvarial defect model for experimentation regarding bone regeneration. J. Periodontal Implant. Sci. **47,** 339-350 https://doi.org/10.5051/jpis.2017.47.5.339

Kim SP, Frey JL, Li Z, Kushwaha P, Zoch ML, Tomlinson RE, Da H, Aja S, Noh HL, Kim JK, et al. (2017): Sclerostin influences body composition by regulating catabolic and anabolic metabolism in adipocytes. Proc. Natl. Acad. Sci. USA **114,** E11238-E11247 https://doi.org/10.1073/pnas.1707876115

Kong X, Zuo Y, Huang YA, Ge J (2019): Adenosine A2a receptor agonist CGS21680 treatment attenuates cardiopulmonary bypass associated inflammatory lung injury in juvenile rats. Mol. Med. Rep. **20,** 117-124 https://doi.org/10.3892/mmr.2019.10235

Koupenova M, Ravid K (2013): Adenosine, adenosine receptors and their role in glucose homeostasis and lipid metabolism. J. Cell Physiol. **228,** 1703-1712 https://doi.org/10.1002/jcp.24352

Kurgan N, Bott KN, Helmeczi WE, Roy BD, Brindle ID, Klentrou P, Fajardo VA (2019): Low dose lithium supplementation activates Wnt/β-catenin signalling and increases bone OPG/RANKL ratio in mice. Biochem. Biophys. Res. Commun. **511,** 394-397 https://doi.org/10.1016/j.bbrc.2019.02.066

Kuroda Y, Maruyama K, Fujii H, Sugawara I, Ko SB, Yasuda H, Matsui H, Matsuo K (2016): Osteoprotegerin regulates pancreatic β-cell homeostasis upon microbial invasion. PLoS One **11,** e0146544 https://doi.org/10.1371/journal.pone.0146544

Li J, Shen X (2019): Oxidative stress and adipokine levels were significantly correlated in diabetic patients with hyperglycemic crises. Diabetol. Metab. Syndr. **11,** 13 https://doi.org/10.1186/s13098-019-0410-5

Livak KJ, Schmittgen TD (2001): Analysis of relative gene expression data using real-time quantitative PCR and the 2−ΔΔCT method. Methods **25,** 402-408 https://doi.org/10.1006/meth.2001.1262

Ma HP, Ma XN, Ge BF, Zhen P, Zhou J, Gao YH, Xian CJ, Chen KM (2014): Icariin attenuates hypoxia-induced oxidative stress and apoptosis in osteoblasts and preserves their osteogenic differentiation potential in vitro. Cell Prolif. **47,** 527-539 https://doi.org/10.1111/cpr.12147

Manjunath S, Sakhare PM (2009): Adenosine and adenosine receptors: Newer therapeutic perspective. Indian J. Pharmacol. **41,** 97 https://doi.org/10.4103/0253-7613.55202

Mediero A, Frenkel SR, Wilder T, He W, Mazumder A, Cronstein BN (2012): Adenosine A2A receptor activation prevents wear particle-induced osteolysis. Sci. Transl. Med. **4,** 135ra65 https://doi.org/10.1126/scitranslmed.3003393

Mediero A, Wilder T, Perez-Aso M, Cronstein BN (2015): Direct or indirect stimulation of adenosine A2A receptors enhances bone regeneration as well as bone morphogenetic protein-2. FASEB J. **29,** 1577 https://doi.org/10.1096/fj.14-265066

Mediero A, Wilder T, Shah L, Cronstein BN (2018): Adenosine A2A receptor (A2AR) stimulation modulates expression of semaphorins 4D and 3A, regulators of bone homeostasis. FASEB J. **32,** 3487 https://doi.org/10.1096/fj.201700217R

Melani A, Corti F, Cellai L, Vannucchi MG, Pedata F (2014): Low doses of the selective adenosine A2A receptor agonist CGS21680 are protective in a rat model of transient cerebral ischemia. Brain Res. **1551,** 59-72 https://doi.org/10.1016/j.brainres.2014.01.014

Mostafavinia A, Amini A, Ghorishi SK, Pouriran R, Bayat M (2016): The effects of dosage and the routes of administrations of streptozotocin and alloxan on induction rate of typel diabetes mellitus and mortality rate in rats. Lab. Anim. Res. **32,** 160-165 https://doi.org/10.5625/lar.2016.32.3.160

Mottalib A, Kasetty M, Mar JY, Elseaidy T, Ashrafzadeh S, Hamdy O (2017): Weight management in patients with type 1 diabetes and obesity. Curr. Diab. Rep. **17,** 1-9 https://doi.org/10.1007/s11892-017-0918-8

Murray CE, Coleman CM (2019): Impact of diabetes mellitus on bone health. Int. J. Mol. Sci. **20,** 4873 https://doi.org/10.3390/ijms20194873

Nadeem A, Fan M, Ansari HR, Ledent C, Jamal Mustafa S (2007): Enhanced airway reactivity and inflammation in A2A adenosine receptor-deficient allergic mice. Am. J. Physiol. Lung Cell Mol. Physiol. **292,** L1335-L1344 https://doi.org/10.1152/ajplung.00416.2006

Nyman JS, Kalaitzoglou E, Bunn RC, Uppuganti S, Thrailkill KM, Fowlkes JL (2017): Preserving and restoring bone with continuous insulin infusion therapy in a mouse model of type 1 diabetes. Bone Rep. **7,** 1-8 https://doi.org/10.1016/j.bonr.2017.07.001

Ohtani M, Oka T, Ohura K (2013): Possible involvement of A2A and A3 receptors in modulation of insulin secretion and β-cell survival in mouse pancreatic islets. Gen. Comp. Endocrinol. **187,** 86-94 https://doi.org/10.1016/j.ygcen.2013.02.011

Pacicca DM, Brown T, Watkins D, Kover K, Yan Y, Prideaux M, Bonewald L (2019): Elevated glucose acts directly on osteocytes to increase sclerostin expression in diabetes. Sci. Rep. **9,** 17353 https://doi.org/10.1038/s41598-019-52224-3

Pellegatti P, Falzoni S, Donvito G, Lemaire I, Di Virgilio F (2011): P2X7 receptor drives osteoclast fusion by increasing the extracellular adenosine concentration. FASEB J. **25,** 1264-1274 https://doi.org/10.1096/fj.10-169854

Pietrzyk B, Smertka M, Chudek J (2017): Sclerostin: Intracellular mechanisms of action and its role in the pathogenesis of skeletal and vascular disorders. Adv. Clin. Exp. Med. **26,** 1283-1291 https://doi.org/10.17219/acem/68739

Qi SS, Shao ML, Sun Z, Chen SM, Hu YJ, Wang HT, Wei TK, Li XS, Zheng HX (2021): Lycopene ameliorates diabetic osteoporosis via anti-inflammatory, anti-oxidation, and increasing Osteoprotegerin/RANKL expression ratio. J. Funct. Foods **83,** 104539 https://doi.org/10.1016/j.jff.2021.104539

Rao Sirasanagandla S, Ranganath Pai Karkala S, Potu BK, Bhat KMR (2014): Beneficial effect of Cissus quadrangularis Linn. on osteopenia associated with streptozotocin-induced type 1 diabetes mellitus in male Wistar rats. Adv. Pharmacol. Pharm. Sci. **2014,** 483051 https://doi.org/10.1155/2014/483051

Romagnoli C, Marcucci G, Favilli F, Zonefrati R, Mavilia C, Galli G, Tanini A, Iantomasi T, Brandi ML, Vincenzini MT (2013): Role of GSH/GSSG redox couple in osteogenic activity and osteoclastogenic markers of human osteoblast-like Sa OS-2 cells. FEBS J. **280,** 867-879 https://doi.org/10.1111/febs.12075

Sabbadin D, Ciancetta A, Deganutti G, Cuzzolin A, Moro S (2015): Exploring the recognition pathway at the human A 2A adenosine receptor of the endogenous agonist adenosine using supervised molecular dynamics simulations. Med. Chem. Comm. **6,** 1081-1085 https://doi.org/10.1039/C5MD00016E

Sun H, Saeedi P, Karuranga S, Pinkepank M, Ogurtsova K, Duncan BB, Stein C, Basit A, Chan JC, Mbanya JC, et al. (2022): IDF Diabetes Atlas: Global, regional and country-level diabetes prevalence estimates for 2021 and projections for 2045. Diabetes Res. Clin. Pract. **183,** 109119 https://doi.org/10.1016/j.diabres.2021.109119

Sun Q, Li J, Gao F (2014): New insights into insulin: The anti-inflammatory effect and its clinical relevance. World J. Diabetes **5,** 89 https://doi.org/10.4239/wjd.v5.i2.89

Suvarna KS, Layton C, Bancroft JD (2018): Bancroft's Theory and Practice of Histological Techniques. Elsevier Health Sciences

Tangvarasittichai S (2015): Oxidative stress, insulin resistance, dyslipidemia and type 2 diabetes mellitus. World J. Diabetes **6,** 456 https://doi.org/10.4239/wjd.v6.i3.456

Wu J, Yan LJ (2015): Streptozotocin-induced type 1 diabetes in rodents as a model for studying mitochondrial mechanisms of diabetic β cell glucotoxicity. Diabetes Metab. Syndr. Obes. **2015,** 181-188 https://doi.org/10.2147/DMSO.S82272

Xing B, Yu J, Zhang H, Li Y (2023): RANKL inhibition: a new target of treating diabetes mellitus? Ther. Adv. Endocrinol. Metab. **14,** 20420188231170754 https://doi.org/10.1177/20420188231170754

Yang Y, Liu G, Zhang Y, Xu G, Yi X, Liang J, Zhao C, Liang J, Ma C, Ye Y, et al. (2020): Linear and non-linear correlations between serum phosphate level and bone mineral density in type 2 diabetes. Front. Endocrinol. **11,** 497 https://doi.org/10.3389/fendo.2020.00497

Zhang J, Corciulo C, Liu H, Wilder T, Ito M, Cronstein B (2017): Adenosine A2a receptor blockade diminishes Wnt/β-Catenin signaling in a murine model of bleomycin-induced dermal fibrosis. Am. J. Pathol. **187,** 1935-1944 https://doi.org/10.1016/j.ajpath.2017.05.005

Zhao Y, Wang HL, Li TT, Yang F, Tzeng CM (2020): Baicalin ameliorates dexamethasone-induced osteoporosis by regulation of the RANK/RANKL/OPG signaling pathway. Drug Des. Devel. Ther. **2020,** 195-206 https://doi.org/10.2147/DDDT.S225516

Received: February 27, 2024
Final version accepted: April 30, 2024